

## RXTE OBSERVATIONS OF A NEW X-RAY TRANSIENT: GRS 1737–31

WEI CUI,<sup>1</sup> W. A. HEINDL,<sup>2</sup> J. H. SWANK,<sup>3</sup> D. M. SMITH,<sup>4</sup> E. H. MORGAN,<sup>1</sup> R. REMILLARD,<sup>1</sup> AND F. E. MARSHALL<sup>3</sup>

Received 1997 May 7; accepted 1997 July 8

### ABSTRACT

We present the results from *RXTE* observations of a new X-ray transient, GRS 1737–31, near the Galactic center during an outburst. Over a span of 2 weeks, the source was seen to vary significantly on timescales down to a few seconds. The rapid flares in the light curves bear resemblance to those observed for Cygnus X-1, a well-known black hole candidate (BHC). The power-density spectrum is also very typical of BHCs in the *hard* (or *low*) state: it is flat below a characteristic break frequency of about 0.03 Hz and becomes roughly a  $1/f$  power law above. The observed X-ray spectrum can be characterized by a simple power law with a photon index of about 1.7 over a broad energy range 2–200 keV, which is remarkably similar to that of Cyg X-1 in the *hard* state. The similarities to Cyg X-1 make GRS 1737–31 a likely BHC. However, unlike most transient BHCs, GRS 1737–31 does not seem to reach a “soft state” even during an outburst. We discuss this phenomenon in light of the comparison to a class of hard X-ray BHCs, including transients GRO J0422+32, V404 Cyg, and GRO J1719–24, and persistent sources 1E1740.7–2942 and GRS 1758–258.

*Subject headings:* binaries: general — stars: individual (GRS 1737–31) — X-rays: stars

### 1. DISCOVERY AND ALL-SKY MONITOR LIGHT CURVE

A new X-ray transient, GRS 1737–31, was discovered during an outburst by the *SIGMA* detector aboard the *Granat* satellite on 1997 March 14 (Sunyaev et al. 1997). The source position was later refined with follow-up observations with the Wide Field Camera on the *BeppoSAX* satellite (Heise 1997) and again with *ASCA* observations (Ueda et al. 1997). In retrospect, a reanalysis of the scans across the region by the Proportional Counter Array (PCA) on the *Rossi X-Ray Timing Explorer* (*RXTE*) showed that the source was in fact detected by the PCA as early as February 17–20 and peaked about 2 weeks later (Marshall & Smith 1997). A brief *RXTE* pointed observation was carried out on 1997 March 21.

The preliminary results from both the *Granat* and *RXTE* observations showed that GRS 1737–31 had a hard X-ray spectrum during the outburst, which was very similar to Cyg X-1 in the *hard* (or *low*) state (Sunyaev et al. 1997; Cui et al. 1997b). The inferred hydrogen column density suggested a source location near the Galactic center (Cui et al. 1997b). Assuming a distance of 8.5 kpc, the 2–150 keV source luminosity was  $1.9 \times 10^{37}$  ergs  $s^{-1}$ , again similar to that of Cyg X-1 (Cui et al. 1997a; Zhang et al. 1997). Similarities between the two extended further to general temporal properties, which suggested that GRS 1737–31 could be a black hole candidate (BHC) as well (Cui et al. 1997b).

The X-ray database of the All-Sky Monitor (ASM) on the *RXTE* satellite (Levine et al. 1996) contains scans of GRS 1737–31, although no data processing was carried out for this source prior to its discovery, since the average flux was below the current threshold for new source detections near the Galactic center. Retrospective ASM analysis was performed, and Figure 1 shows a light curve of the source in the ASM energy band (1.3–12 keV) in 2 day bins (excluding data points

with error bars greater than 1.0 counts  $s^{-1}$ ). The light curve shows that GRS 1737–31 started an outburst some time after 1997 February 14 (MJD 50493), in good agreement with the PCA scan results. Averaging over a period MJD 50,100–50,400 gives an ASM flux of approximately 7.6 mcrab. Further pointed observations were made with the PCA and the High Energy X-Ray Timing Experiment (HEXTE) aboard *RXTE*. In the following section, we present the results from our detailed timing and spectral analyses of the pointed observations.

### 2. POINTED RXTE OBSERVATIONS AND ANALYSES

The details of the observations are summarized in Table 1, with the pointings slightly offset from the *ASCA* position in order to ensure that another source (X1732–304) was outside of the field of view (FOV). The PCA and HEXTE share a common  $1^\circ$  FOV (FWHM). The PCA (Jahoda et al. 1996) consists of five nearly identical large-area proportional counter units (PCUs), with a total collecting area of about 6500  $cm^2$ . All five PCUs were used for the first two observations. However, shortly after the last one started, one PCU was turned off for instrument safety reasons. The PCA covers an energy range 2–60 keV with a moderate energy resolution ( $\sim 18\%$  at 6 keV). The HEXTE has a total effective area of about 1600  $cm^2$  in two clusters. It covers a wide energy range from about 15 to 250 keV with an energy resolution of about 16% at 60 keV. The two clusters alternately rock on and off the source to provide nearly simultaneous background measurement.

Because GRS 1737–31 is so close to the Galactic center, we were concerned about contamination by the “Galactic ridge” emission (e.g., Worrall et al. 1982; Warwick et al. 1985; 1988; Koyama et al. 1986). Since this diffuse component is not included in the PCA background model, a set of off-source pointings were made in the immediate vicinity of the source (see Table 2 for details), in order to model accurately the PCA background.

<sup>1</sup> Center for Space Research, Massachusetts Institute of Technology, Cambridge, MA 02139; cui@space.mit.edu.

<sup>2</sup> Center for Astrophysics and Space Sciences, University of California, San Diego, La Jolla, CA 92093.

<sup>3</sup> NASA/Goddard Space Flight Center, Code 662, Greenbelt, MD 20771.

<sup>4</sup> Space Sciences Laboratory, University of California, Berkeley, Berkeley, CA 94720.

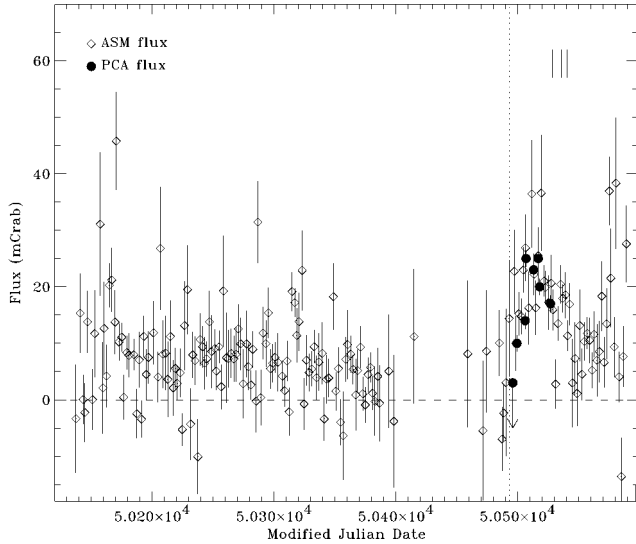


FIG. 1.—ASM light curve of GRS 1737–31 in 2 day bins; 1 crab corresponds to about  $75 \text{ counts s}^{-1}$  in the ASM band (1.3–12 keV). The dotted line shows roughly when the outburst started. Also shown are the PCA slew measurements in the energy range 2–10 keV (see text), with the  $1 \sigma$  error being conservatively estimated to be 1.5 mcrab, which is dominated by the uncertainty in the background. The ticks near the top indicate when the pointed *RXTE* observations were carried out.

### 2.1. Timing Analysis

Only the PCA data are used here. GRS 1737–31 displayed large X-ray variability with occasional flares that lasted a few seconds. Figure 2 shows a typical example of the light curve, made from the “Standard1” data with a 1/8 s timing resolution.

High timing resolution data ( $\sim 1 \mu\text{s}$ ) are available through two “goodXenon” modes. Using the Fast Fourier transform (FFT) technique, a search for high-frequency features (e.g., quasi-periodic oscillations) was carried out at frequencies of up to a few kilohertz, but none were detected. In fact, most of the power lies below a few hertz. For a better low-frequency coverage, we broke up the “Standard1” data into 256 s segments for each observation, performed FFT on each segment, and averaged the results. Figure 3 shows the average power-density spectra (PDS). Note that the power density is expressed in terms of the fractional rms amplitude squared, which is defined as Leahy normalized power (with Poisson noise power subtracted) divided by the mean source count rate (van der Klis 1995). Instrumental artifacts due to electronic dead time and very high energy events (Zhang et al. 1996) were taken into account.

There is no apparent temporal evolution between the observations: the PDS is flat below about 0.03 Hz and drops roughly as a simple  $1/f$  power law above. Integrating over a range 0–4 Hz, the fractional rms variability is about 30% for

TABLE 1  
*RXTE* OBSERVATIONS OF GRS 1737–31<sup>a</sup>

OBSERVATION	TIME (UT)	LIVE TIME (s)	
		PCA	HEXTE <sup>b</sup>
1 .....	1997 Mar 21 16:36:00–17:37:00	3248	1972
2 .....	1997 Mar 28 12:16:00–16:04:00	5440	2571
3 .....	1997 Apr 02 14:44:00–20:01:00	10640	5966

<sup>a</sup> Pointing coordinates: R.A. =  $17^{\text{h}}40^{\text{m}}24^{\text{s}}$ , decl. =  $-31^{\circ}00'00''$ , epoch J2000.

<sup>b</sup> Both clusters are included.

TABLE 2

PCA BACKGROUND OBSERVATIONS ON 1997 MARCH 28

Observation	R.A. <sup>a</sup>	Decl. <sup>a</sup>	Time (UT)	Exposure (s)
1 .....	266°20	–31°00	13:28:00–13:39:28	608
2 .....	265°00	–33°00	13:39:29–13:51:59	736
3 .....	264°10	–32°10	13:52:00–14:02:59	576

<sup>a</sup> Epoch J2000.

all observations. It is larger than our preliminary estimate (Cui et al. 1997b) because we are now including the “Galactic Ridge” emission in the background modeling.

### 2.2. Spectral Analysis

On-source time intervals were selected from the raw light curves and were used to extract an X-ray spectrum for each observation. We simultaneously fitted the individual PCA spectra and HEXTE cluster spectra with a simple power law plus a Gaussian component (to model a line feature at 6.6–6.7 keV that is apparent in the raw spectra). The relative normalization between the PCA and HEXTE was allowed to vary because of the uncertainty in their relative effective areas. The results are summarized in Table 3.

In fitting the PCA and HEXTE spectra, we alternately used the individual PCA off-source pointings as well as the average result to represent the PCA background spectrum. The variation in the background ( $<20\%$  in total count rate) provides a realistic estimate of the systematic uncertainty for the analysis, since this effect dominates the statistical and any PCA calibration uncertainties. The “best-fit” parameters were derived by using the average off-source spectrum as the PCA background, and the uncertainties represent the range of each parameter derived using different off-source spectra.

The simple model characterizes the observed X-ray spectrum reasonably well over a broad energy range 2–200 keV, as indicated by the small reduced  $\chi^2$  values (which are based on only the statistical uncertainty of the data). As an example, Figure 4 shows the spectrum from observation 2, with the

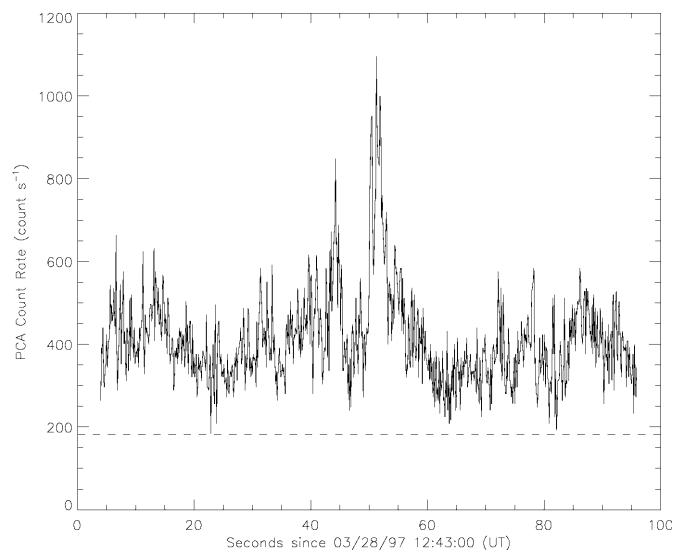


FIG. 2.—A segment of the PCA light curve of GRS 1737–31 from the second observation (see Table 1). The time bin size is 0.125 s. The dashed line indicates the average background count rate.

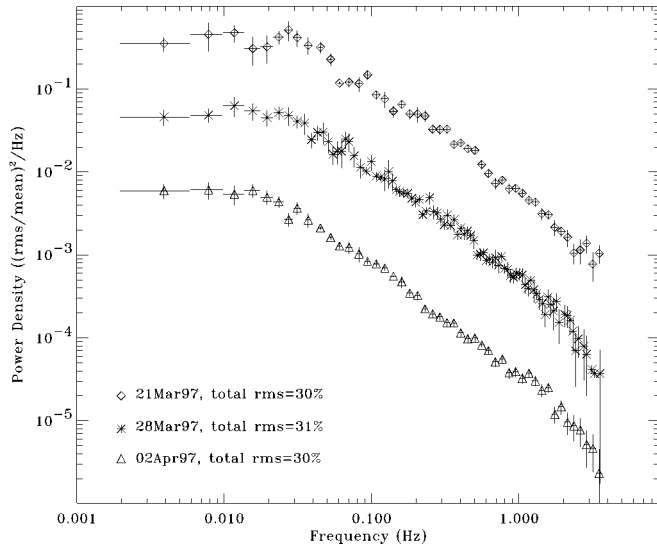


FIG. 3.—Power-density spectra of GRS 1737–31. They are derived over the entire PCA band. For clarity, the lower two curves have been shifted down by a factor by 10 and 100, respectively.

average off-source spectrum subtracted, along with the best-fit model and residual spectrum. Although no significant emission is apparent above about 130 keV from the figure, the source can be detected up to about 200 keV when combining data from all observations.

To investigate the presence of a possible ultrasoft component, typical for BHCs, we added a blackbody component to the model and refitted the data. Only in some of the cases (in which different off-source spectra were used for the PCA background) was a nonzero normalization for this component obtained, providing slightly improved fits. In those cases, the blackbody temperature is in the range 0.9–1.5 keV, and the soft component accounts for less than about 10% of the intrinsic 2–10 keV flux. Neither was an ultrasoft component needed to fit the *ASCA* data (Ueda et al. 1997).

### 3. DISCUSSION

Both the light curves and PDS of GRS 1737–31 during the outburst are remarkably similar to Cyg X-1 in the *hard* state (see review by van der Klis 1995 and references therein). Recent works on Cyg X-1 (Cui et al. 1997a, 1997c, 1997d) showed that the white noise (i.e., the flat portion at low frequency) may be intrinsic to the source, originating in the statistical fluctuation associated with the accretion process near the black hole, where the dynamical timescale is very short. It was speculated that the intrinsic PDS is then modified by the scattering process occurring in a hot electron corona,

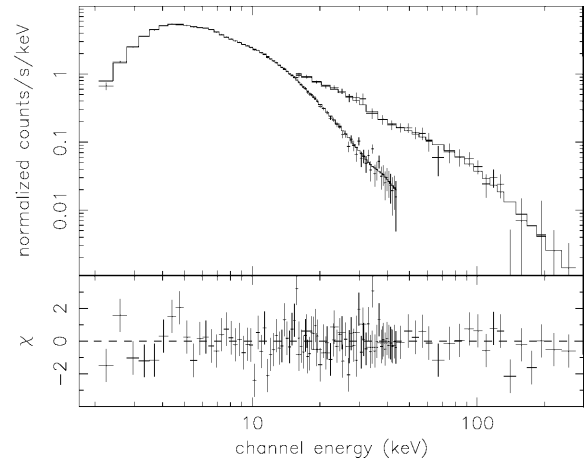


FIG. 4.—Joint PCA/HEXTE spectrum of GRS 1737–31 obtained from the second observation. Note that the average off-source spectrum is subtracted as the PCA background (see text). For clarity, five PCU spectra are co-added, and so are the HEXTE cluster spectra. The errors shown are purely statistical. The solid histogram shows the best-fit model.

which acts as a low-pass filter. The break frequency is simply determined by the characteristic photon escape time from the corona (thus its physical size). If GRS 1737–31 is also a black hole binary, then the observed break frequency would imply a similar corona size to that of Cyg X-1 in the hard state.

The observed X-ray continuum of GRS 1737–31 can be characterized by a simple power law with a photon index of about 1.7 over an energy range of 2–200 keV. The power-law spectrum is very typical of BHCs and used to be considered as one of their defining signatures. In fact, this photon index is also typical for Cyg X-1 in the hard state. For Cyg X-1, the power-law spectrum is thought to be the product of inverse Comptonization of the soft photons in the region by the hot corona (e.g., Shapiro, Lightman, & Eardley 1976). Similar physical processes may also be involved in GRS 1737–31. However, unlike most transient BHCs, GRS 1737–31 does not seem to reach a “soft state” even during an outburst. This phenomenon was also observed for persistent BHCs 1E1740.7–2942 and GRS 1758–258.

One of the important spectral characteristics for a typical BHC is the presence of a prominent ultrasoft component, which is thought to be the emission from the inner edge of the accretion disk. It has been a long-standing puzzle in black hole studies why such a component has *never* been seen for some of the known BHCs, such as transients V404 Cyg, GRO J0422+32, and GRO J1719–24, and persistent sources 1E1740.7–2942 and GRS 1758–258. The lack of a strong soft component seems to indicate that GRS 1737–31 is perhaps

TABLE 3  
RESULTS OF SPECTRAL ANALYSIS<sup>a</sup>

Observation	$N_{\text{H}}^{\text{b}}$	$\alpha$	$N_{\alpha}^{\text{c}}$	$E_{\text{c}}$ (keV)	$E_{\sigma}$ (keV)	EW (eV)	Flux <sup>d</sup>	$\chi^2_{\text{r}}/\text{dof}$
1 .....	$5.6^{+0.4}_{-0.8}$	$1.69^{+0.03}_{-0.07}$	$1.19^{+0.07}_{-0.18}$	$6.61^{+0.00}_{-0.01}$	$0.25^{+0.29}_{-0.08}$	$61^{+24}_{-20}$	$2.3^{+0.3}_{-0.2}$	$1.3^{+0.3}_{-0.2}/488$
2 .....	$5.5^{+0.6}_{-1.1}$	$1.68^{+0.05}_{-0.09}$	$0.94^{+0.07}_{-0.18}$	$6.62^{+0.00}_{-0.02}$	$0.3^{+0.6}_{-0.1}$	$83^{+39}_{-39}$	$1.8^{+0.3}_{-0.1}$	$1.2^{+0.2}_{-0.1}/488$
3 .....	$6.3^{+0.7}_{-1.1}$	$1.76^{+0.05}_{-0.10}$	$0.89^{+0.07}_{-0.18}$	$6.7^{+0.0}_{-0.1}$	$0.3^{+0.4}_{-0.1}$	$88^{+27}_{-36}$	$1.3^{+0.2}_{-0.2}$	$1.5^{+0.4}_{-0.4}/408$

<sup>a</sup> Errors represent the range of parameters derived by using individual off-source pointings as the background.

<sup>b</sup> H I column density along the line of sight, in units of  $10^{22} \text{ cm}^{-2}$ .

<sup>c</sup> Power-law normalization, in units of  $10^{-1} \text{ photons cm}^{-2} \text{ s}^{-1} \text{ keV}^{-1}$  at 1 keV.

<sup>d</sup> Observed 2–200 keV flux, in units of  $10^{-9} \text{ ergs cm}^{-2} \text{ s}^{-1}$ .

another one of this type. Recently, Zhang, Cui, & Chen (1997) argued that the strength of the ultrasoft component may be directly related to the spin of the black hole, which determines the location of the last stable orbit, since there are no known processes to keep the accretion disk from extending close to the last stable orbit in the high state. They speculated that the absence of an ultrasoft component may indicate the presence of a rapidly rotating black hole in the system with a retrograde disk. In such cases, the last stable orbit, and thus the inner edge of the disk, is farther away from the black hole than the nonrotating ones, so the temperature of the region may be too low for the emission to be detected by current experiments.

The inferred hydrogen column density for GRS 1737–31 is in a range  $(4.8\text{--}7.0) \times 10^{22} \text{ cm}^{-2}$ , in excellent agreement with the results from the *ASCA* observation (Ueda et al. 1997). Therefore, GRS 1737–31 is likely to be near the Galactic center, again similar to 1E1740.7–2942 and GRS 1758–258. Unlike in those cases, however, no radio or infrared counterparts have been identified for GRS 1737–31.

The “Galactic ridge” emission is known to show strong iron emission lines at about 6.7 keV (e.g., Koyama et al. 1986; Koyama 1989; Yamauchi et al. 1990; Koyama et al. 1996). Imperfect background subtraction could lead to the appear-

ance of an iron line in the net spectrum. We estimated that the line fluxes in the  $1^\circ$  FOV were roughly 6.8, 4.6, and  $5.5 \times 10^{-4}$  photons  $\text{s}^{-1} \text{ cm}^{-2}$ , respectively, from the PCA background fields 1, 2, and 3. These are consistent with the *ASCA* measurements (M. Sakano & K. Koyama 1997, private communication), using fields much closer to GRS 1737–31 from the image (Ueda et al. 1997). Therefore, the PCA off-source pointings seem to provide a good estimate of the local diffuse flux. The source spectrum obtained with the PCA appears to contain residual iron-line emission. The equivalent widths in Table 3 correspond to line fluxes of  $2.9_{-1.2}^{+1.0}$ ,  $3.0_{-1.1}^{+1.2}$ , and  $2.5_{-1.0}^{+1.0} \times 10^{-4}$  photons  $\text{s}^{-1} \text{ cm}^{-2}$ . The line could be due to the fluorescent emission from highly ionized iron atoms associated with the source. However, this detection should be taken with reservation, because of the uncertainty in the PCA calibration.

We gratefully acknowledge the effort by the staff at the *RXTE* Science Operation Center for making flexible mission operation a reality. This work is supported in part by NASA contracts NAS 5-30612 and NAS 5-30720.

#### REFERENCES

- Cui, W., Heindl, W. A., Rothschild, R. E., Zhang, S. N., Jahoda, K., & Focke, W. 1997a, *ApJ*, 474, L57  
 Cui, W., Morgan, E. H., Heindl, W. A., Swank, J. H., & Smith, D. M. 1997b, *IAU Circ.* 6604  
 Cui, W., Zhang, S. N., Focke, W., & Swank, J. H. 1997c, *ApJ*, 484, 383  
 Cui, W., Zhang, S. N., Heindl, W. A., Rothschild, R. E., Jahoda, K., Focke, W., & Swank, J. H. 1997d, *Proc. 2d Integral Workshop, The Transparent Universe*, ed. C. Winkler et al. (ESA-SP 382), 209  
 Heise, J. 1997, *IAU Circ.* 6606  
 Jahoda, K., Swank, J. H., Giles, A. B., Stark, M. J., Strohmayer, T., Zhang, W., & Morgan, E. H. 1996, *Proc. SPIE*, 2808, 59  
 Koyama, K. 1989, *PASJ*, 41, 665  
 Koyama, K., Maeda, Y., Sonobe, T., Takeshima, T., Tanaka, Y., & Yanauchi, S. 1996, *PASJ*, 48, 249  
 Koyama, K., Makishima, K., Tanaka, Y., & Tsunemi, H. 1986, *PASJ*, 38, 121  
 Levine, A., et al. 1996, *ApJ*, 469, L33  
 Marshall, F. E., & Smith, D. M. 1997, *IAU Circ.* 6603  
 Shapiro, S. L., Lightman, A. P., & Eardley, D. 1976, *ApJ*, 204, 187  
 Sunyaev, R., Churazov, E., Revnivtsev M., Trudolyubov, S., Vargas, M., Paul, J., Roques J.-P., & Jourdain, E. 1997, *IAU Circ.* 6599  
 Ueda, Y., et al. 1997, *IAU Circ.* 6627  
 van der Klis, M. 1995, in *X-Ray Binaries*, ed. W. H. G. Lewin, J. van Paradijs, & E. P. J. van den Heuvel (Cambridge: Cambridge Univ. Press), 252  
 Warwick, R. S., Norton, A. J., Turner, M. J. L., Watson, M. G., & Willingale, R. 1988, *MNRAS*, 232, 551  
 Warwick, R. S., Turner, M. J. L., Watson, M. G., & Willingale, R. 1985, *Nature*, 317, 218  
 Worrall, D. M., Marshall, F. E., Boldt, E. A., & Swank, J. H. 1982, *ApJ*, 255, 111  
 Yamauchi, S., Kawada, M., Koyama, K., Kunieda, H., & Tawara, T. 1990, *ApJ*, 365, 532  
 Zhang, S. N., Cui, W., & Chen, W. 1997, *ApJ*, 482, L155  
 Zhang, S. N., Cui, W., Harmon, B. A., Paciesas, W. S., Remillard, R. E., & van Paradijs, J. 1997, *ApJ*, 477, L95  
 Zhang, W., Morgan, E. H., Jahoda, K., Swank, J. H., Strohmayer, T. E., Jernigan, G., & Klein, R. I. 1996, *ApJ*, 469, L29